Kinetically and Thermodynamically Controlled Cross-Linking in Sustainable Digital Light Processing Resins: Enabling Thermoset Reprocessing via Thermal Levelling Effect

Yi Ting Chong,[1] Suxi Wang,[1] Sirawit Pruksawan,[1] Zhuang Mao Png,[2*] Qiang Zhu,[1] Zibiao Li,[2,3] FuKe Wang[1*]

[1] Institute of Materials Research and Engineering, A*STAR (Agency for Science, Technology and Research), Fusionopolis Way, Innovis, #08-03, Singapore 138634, Republic of Singapore

[2] Institute of Sustainability for Chemicals, Energy and Environment (ISCE[2]), A*STAR (Agency for Science, Technology and Research), 1 Pesek Road, Jurong Island, Singapore 627833, Republic of Singapore

[3] Department of Materials Science and Engineering, National University of Singapore, 9 Engineering Drive 1, Singapore 117576, Republic of Singapore

Corresponding email: png_zhuang_mao@isce2.a-star.edu.sg; wangf@imre.a-star.edu.sg

Abstract

High-performance resins are essential for DLP 3D printing, yet most are thermosetting and lack re-processability. Recently developed covalent adaptive networks (CANs) address this limitation but its reliance on specialized monomers hinders scalability and practical application. Herein, we report a 3D-printable resin formulated with isobornyl acrylate, a 1,2-diol-based boronic ester cross-linker (<4%), and tetradecanol as a trans-borylesterification mediator. At room temperature, tetradecanol remains unreactive, preserving a rigid thermoset matrix while forming micro-elastic domains that dissipate impact energy, achieving an 8600% increase in toughness with 15% tetradecanol. During hot pressing, the thermal levelling effect kinetically drives dynamic bond exchange, converting the thermoset into thermoplastic material. Upon cooling, the reaction becomes thermodynamically controlled again, reestablishing the thermoset polymer network and recovering mechanical properties. This resin uniquely transitions to a thermoplastic state only during reprocessing, reverting to a durable thermoset upon cooling, enabling sustainable, high-performance DLP printing with end-of-life reusability.

3D-printing technologies have revolutionized the manufacturing landscape, enabling rapid prototyping, complex geometries, and customized fabrication with less waste.[1, 2] Among these printing technologies, Digital Light Processing (DLP) has emerged as a prominent technique to quickly fabricate intricate structures with fine product surface.[3-5] However, resins used in DLP printing typically comprise multifunctional monomers or oligomers that form printed thermosets networks.[6-8] While thermosets often possess excellent mechanical properties and thermal stability, they are typically non-re-processability due to their permanently crosslinked structure.[9-11] With sustainability becoming an important focus in materials science, the development of sustainable resins which are reprocessable and recyclable is now essential for broader adoption of this DLP printing in industry to improve material circularity.[12-16]

In light of this challenge, various strategies have been applied to develop "re-workable" DLP resins.[17, 18] For instance, thermoplastic resins which can be remelted and reshaped have been developed.[19-22] However, most of these resins suffer from low glass transition temperatures (T_g), resulting in soft printed parts which may redissolve into the monomer bath during printing, causing print failures and deformation. Additionally, thermoplastic resins typically exhibit inferior mechanical properties compared to thermosets. As such, balancing re-processability with mechanical performance remains a significant challenge in the development of sustainable DLP resins.[19, 20] Recently, there have been growing attention towards incorporating dynamic covalent chemistry (DCC) in resin formulations.[9, 10, 23-28] Unlike the permanent crosslinks of thermosets, crosslinks using DCC can be broken and reformed under specific conditions, allowing for re-processability, reconfiguration, and self-healing properties. This allows the resultant resin to remain thermoset-like while being reprocessable.[29] While promising, DCC-based resins can be complex to synthesize and may

require precise control of reprocessing conditions or extra solvent, which limit their practical application.

Herein, we introduce an alternate strategy to develop a re-processable thermoset resin for DLP printing by leveraging the thermal levelling effect to control functional group exchange, using mono-alcohol as a modulator. The reaction of 1,2- or 1,3-diols with boronic acids is known to be entropically and thermodynamically favoured over reaction with mono-alcohols due to an overall increase in number of participating molecules (Eq. 1).[30, 31]

$$\Delta G = \Delta H - T\Delta S \quad \text{(Eq. 1)}$$

Where ΔG is the Gibbs Free Energy change of reaction, ΔH is the enthalpy change of reaction, ΔT is the absolute temperature, and ΔS is the entropic change of reaction.

However, according to the Arrhenius equation (Eq. 2), the rate of a reaction increases exponentially with temperature.

$$k = Ae^{\frac{-E_a}{RT}} \quad \text{(Eq. 2)}$$

Where k is the reaction rate constant, A is the pre-exponential factor, Ea is the activation energy, R is the gas constant, and T is the absolute temperature.

According to this equation (the factor $e^{\frac{-E_a}{RT}}$), as temperature increases, the rate of any reaction increases as the fraction of molecules with enough energy to overcome the activation energy barrier (Ea) increases. As a result, despite diol derived boronic esters being the thermodynamic product, the reactivity of mono-alcohols also increases as temperature increases. At the same time, the reactivity of diols, already active at room temperature, becomes less sensitive to further temperature increases. This convergence of reactivity at higher temperatures effectively "levels" the difference between diols and mono-alcohols kinetically, resulting in mono-alcohol products being observable at elevated temperatures. As

the system is cooled, thermodynamic factors once again dominates and the diol derived product reforms.[32]

In the present work, as shown in Figure 1a, when isobornyl acrylate (**IBA**) is copolymerized with 1,4-phenylenebis(1,3,2-dioxaborolane-2,4-diyl)-bis(methylene) diacrylate (**PDBDA**) during UV curing in DLP 3D printing, a thermoset is obtained with **PDBDA** functioning as a diboronate ester (**BE**) cross-linker. Additionally, a certain amount of 1-tetradecanol ($C_{14}OH$) is added as a mediator. At room temperature, boronic acid forms stronger **BE** bonds with the 1,2-dioxolan, while there is almost no reaction with $C_{14}OH$, the mono-alcohol. Consequently, the poly(**IBA-PDBDA**) thermoset with **BE** cross-links dominates the structure (Figure 1b (i)). However, when the temperature increases, the thermal levelling effect narrows the reactivity gap between boron acid with the diols and mono-alcohol. Given the large amount of $C_{14}OH$ in the system, with kinetic control taking precedence over thermodynamics, most of the boronic acid reacts with the mono-alcohol instead of the 1,2-dioxolan, leading to the breakdown of cross-linkage transitioning the polymer into a molten thermoplastic state (Figure 1b (ii)). This polymer can then be re-processed into different shapes. Conversely, when the reprocessed product is cooled to room temperature, the reaction between boronic acid and alcohol becomes thermodynamically controlled again, with boronic acid preferentially reacting with 1,2-dioxolan, leading to the reformation of the 3D cross-linked thermoset structure (Figure 1b (iii)). In practical applications, this means that the printed thermoset (Figure 1c(i)) can be melted at a high temperature (Figure 1c(ii)) and then reprocessed like a thermoplastic into different shapes. Upon cooling, the thermosetting properties such as tensile strength are restored (Figure 1c (iii)).

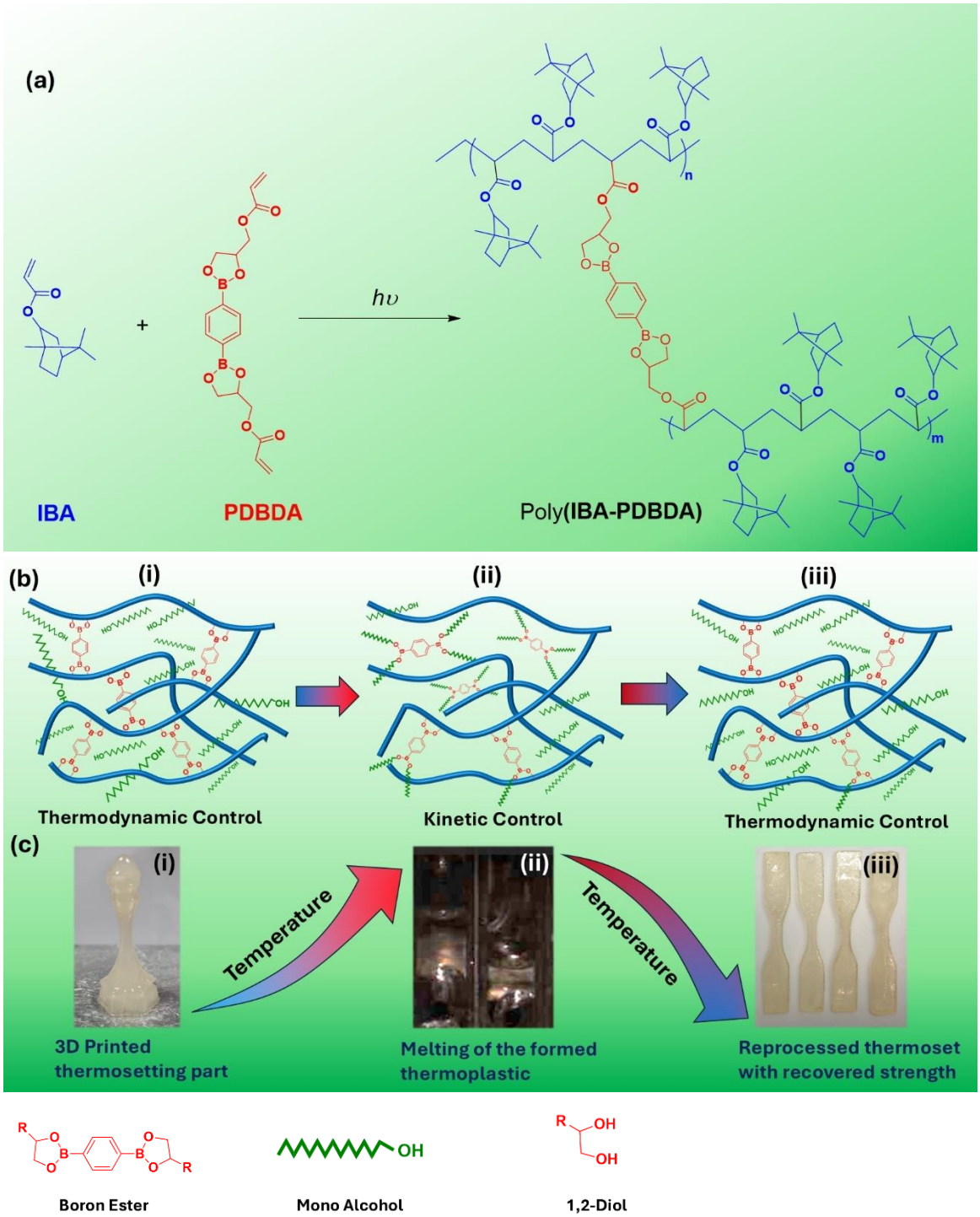

Figure 1. **Mechanism illustration of the thermal levelling effect in poly(IBA-PDBDA) with tetradecanol for sustainable resin construction**. (a) Synthetic route for the formation of poly(**IBA-PDBDA**). (b) Transition between thermos-kinetic and thermodynamic control of dynamic covalent bonding (DCC) within the system. (c) Practical changes in thermosetting and thermoplastic properties during and after the reprocessing cycle.

Dynamic covalent bonds formed through transesterification reactions between boronic esters and various types of diols have been extensively studied and applied in the development of self-healing polymer systems.[24, 30, 33-37] However, the transesterification of boronic esters with mono-alcohols has rarely been explored, primarily due to the decreased entropy and thus the increased Gibbs free energy. We hypothesised that at elevated temperatures with a high concentration of mono-alcohol, the reaction between boronic esters and alcohols become kinetically controlled due to the thermal levelling effect, with boron esters of the mono-alcohols being formed. To test this hypothesis, we used a small molecule model system comprising diboronate ester (**BE**) and the mono-alcohol 1-tetradecanol ($C_{14}OH$), and employed ^{1}H-NMR spectroscopy to monitor the progress of transesterification at different temperatures.

To simulate the reprocessing condition of the printed resin, the solid mixture of **BE** and $C_{14}OH$ with a molar ratio of 1/28 was initially heated at 120 °C for 20 minutes and subsequently cooled down and maintained at room temperature for 1, 4, and 7 days (Figure 2b). Due to the reversibility of the transesterification process, the reaction mixture comprises an equilibrium mixture of boronic esters, including the ethylene glycol diboronate ester, mono- and di-substituted $C_{14}OH$ boronic esters. Figure 2a displays the evolution of ^{1}H NMR spectra of the reaction mixture at different stages of the process, with the corresponding peak intensity ratio shown in Figure 2c. Prior to the reaction, the ^{1}H NMR spectrum of **BE** exhibited a singlet peak at 7.86 ppm relating to the aromatic protons of the 1,4-phenylene unit (Ha), as well as a singlet peak at 4.38 ppm corresponding to the protons on the 1,3-dioxolane ring (Hb). The initial peak intensity ratio of Hb to Ha was 2.00 : 1. Upon heating with a large excess amount of $C_{14}OH$ at 120 °C, multiplet aromatic proton signals were detected within the chemical shift range of 7.5 ~ 7.9 ppm, and a doublet Hb peak was observed at 4.37 ppm. The peak intensity ratio of Hb to Ha was significantly reduced to 0.48 : 1, indicating that the

dioxolane ring was broken as a result of transesterification at high temperature with a high concentration of $C_{14}OH$, which is a kinetic controlled process. As expected, the ratio was found to be dependent on the reaction temperature. When **BE** was heated with $C_{14}OH$ at a lower temperature (e.g., 90 °C), the ratio was approximately 1.23 : 1, indicating a low degree of transesterification. However, increasing the reaction temperature to 140 °C reduced the ratio to 0.42 : 1 (Table S1), suggesting a higher degree of transesterification at elevated temperatures. Notably, the ratio did not change significantly beyond 120 °C, indicating that this temperature is high enough for effective transesterification. It is worth mentioning that lower amounts of $C_{14}OH$ were also examined to trigger the reaction, though the Hb to Ha ratio did not decrease obviously (Table S1 and Figure S1, S2, Supporting Information), demonstrating that the excessive concentration of the mono-alcohol is crucial for this kinetic regulated process. Subsequently, after cooling down and storage of the reaction mixture at room temperature over a period of 1 to 7 days, the NMR spectra revealed a steady increase in the Hb to Ha ratio from 0.60 : 1 to 1.80 : 1, as well as a transition from multiplet aromatic proton peaks to a prominent singlet peak. This evolution is ascribed to the thermodynamically controlled mechanism that resulted in the reformation of the more stable ethylene glycol boronic ester.

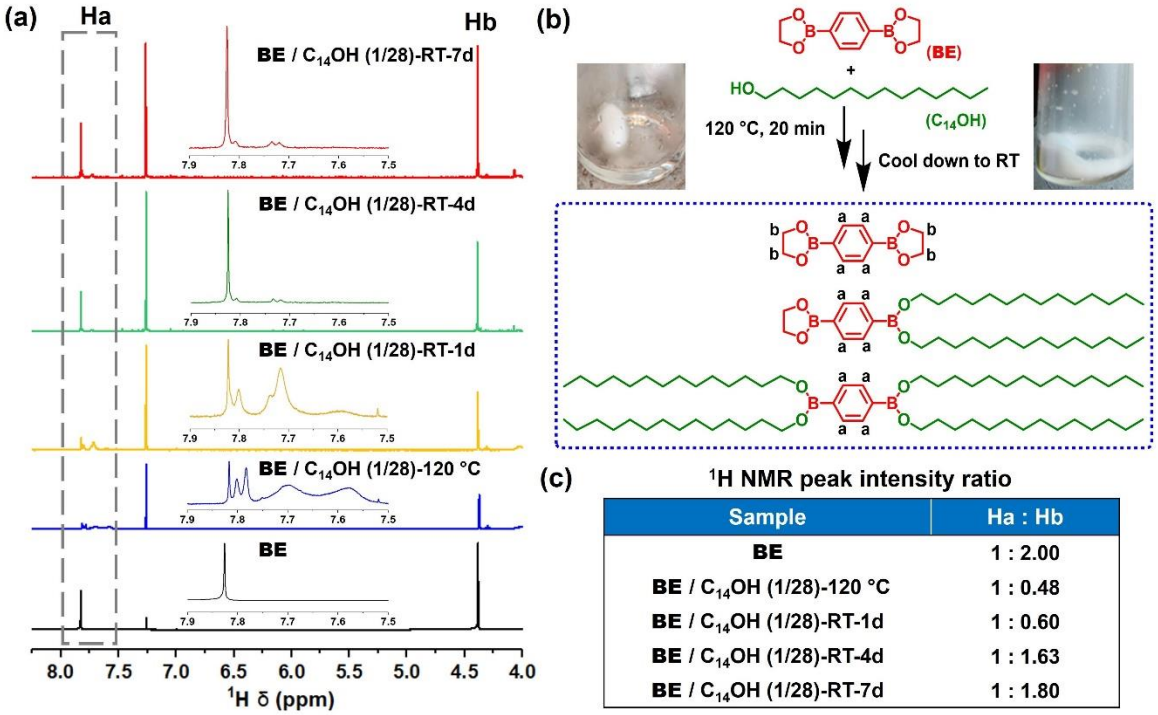

Sample	Ha : Hb
BE	1 : 2.00
BE / C_{14}OH (1/28)-120 °C	1 : 0.48
BE / C_{14}OH (1/28)-RT-1d	1 : 0.60
BE / C_{14}OH (1/28)-RT-4d	1 : 1.63
BE / C_{14}OH (1/28)-RT-7d	1 : 1.80

Figure 2. (a) ^{1}H NMR spectra of the **BE** and C_{14}OH reaction mixture (with a molar ratio of 1/28) obtained after heat treatment at 120 °C, and storage at room temperature for 1, 4 and 7 days. (b) Schematic showing the solid-state reaction process between **BE** and C_{14}OH. (c) ^{1}H NMR peak intensity ratio of boronic ester mixtures at different reaction stages (Ha: aromatic protons, Hb: protons on the 1,3-dioxolane ring).

As shown in Figure 1, the base resin consists primarily of isobornyl acrylate (**IBA**), with 1,4-phenylenebis(1,3,2-dioxaborolane-2,4-diyl)methylene diacrylate (**PDBDA**) serving as the cross-linker. The formed thermosetting poly(**IBA-PDBDA**) exhibits brittle characteristics, which limit its processability.[38, 39] We attempted to tune the thermosetting property of poly(**IBA-PDBDA**) by introducing ethylene glycol, a 1,2-diol that can interact with boronic ester. However, the polymer formed was sticky, likely due to two factors: (1) ethylene glycol, being a low-viscosity liquid, softened the resulting polymer when added in high amounts; and (2) the 1,2-diol structure tends to react with **PDBDA** at room temperature, disrupting the thermosetting polymer network and reducing stability.

To address this issue, we systematically investigated mono-alcohols of varying chain lengths and found that short-chain alcohols (e.g., octanol) resulted in gel-like cured products,

rendering them unsuitable for DLP printing. In contrast, longer-chain alcohols (e.g., hexadecanol) solidified the resin at room temperature, making them unprintable as well. Hence, the mono-alcohol, tetradecanol ($C_{14}OH$), was incorporated as a functional additive to enable group exchange reactions at elevated temperatures, allowing the polymer to exhibit thermoplastic properties at high temperatures. To catalyze this reaction, 1% 4-Dimethylaminopyridine (DMAP) was added. The specific resin formulation is summarized in Table 1.

The impact of $C_{14}OH$ content on polymerization and the resulting polymer structure was investigated by varying its concentration from 0% to 20% in poly(**IBA-PDBDA**) with 2% diboronate ester (**BE**) cross-linker. FT-IR analysis (Figure 3a) confirmed successful photopolymerization, indicated by the near disappearance of the C=C bond vibration at 1635 cm^{-1}, associated with acrylate groups. The addition of $C_{14}OH$ did not interfere with this process, as evidenced by the preservation of the 1635 cm^{-1} peak.

Table 1: Composition and properties of resins examined in the optimization.

Entry No.	Resin component[a]	$C_{14}OH$ (g)	**PDBDA** (g)	Properties
1	2**BE**	-	0.1	Brittle
2	2**BE** – 4 $C_{14}OH$	0.22	0.1	Brittle
3	2**BE** – 10 $C_{14}OH$	0.52	0.1	Brittle
4	2**BE** – 15 $C_{14}OH$	0.77	0.1	Hard Solid
5	2**BE** – 20 $C_{14}OH$	1.00	0.1	Soft
6	0**BE** – 15 $C_{14}OH$	0.77	0	Hard Solid
7	1**BE** – 15 $C_{14}OH$	0.77	0.05	Hard Solid
8	4**BE** – 15 $C_{14}OH$	0.77	0.2	Hard Solid

[a]*All resins also include **IBA** (5 g) as the base material, DMAP (1%, 0.05 g) as catalyst, and DPO (2%, 0.1 g) as the photo-initiator.*

However, increasing the $C_{14}OH$ content led to a corresponding increase in peaks at 3322 cm^{-1} (OH stretching vibration) and at 2915 cm^{-1} and 2848 cm^{-1} (aliphatic -CH_2 stretching vibrations), which signifies the integration of $C_{14}OH$ into the polymer matrix. The presence of $C_{14}OH$ did not affect the C=C bond conversion, indicating that it has minimal impact on the polymerization kinetics of poly(**IBA-PDBDA**).

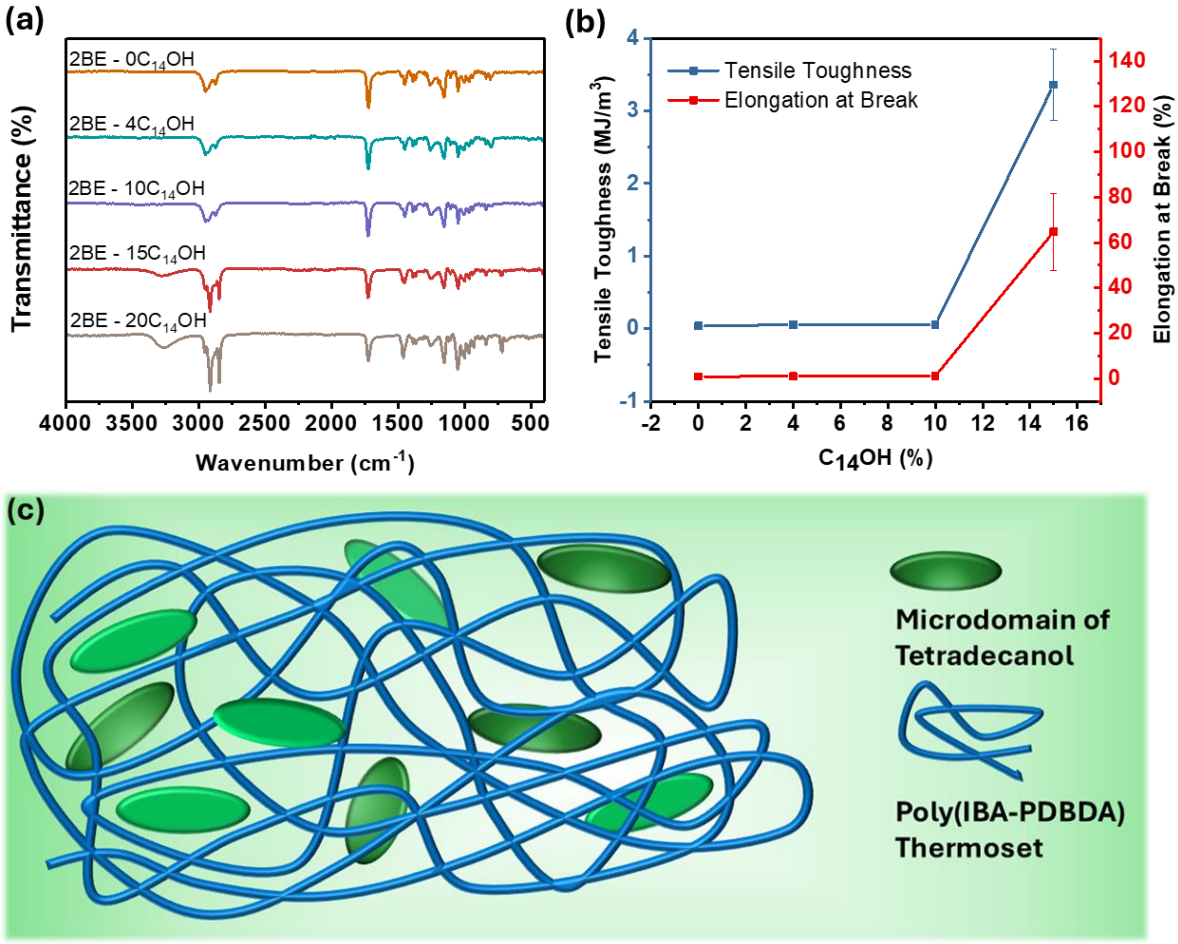

Figure 3. **Role of $C_{14}OH$ in the system**. (a) FT-IR spectra of poly(**IBA-PDBDA**) with 2% **BE** at varying $C_{14}OH$ contents. (b) Tensile toughness and elongation of poly(**IBA-PDBDA**) as a function of $C_{14}OH$ content. (c) Proposed mechanism illustrating how assembled $C_{14}OH$ microdomains contribute to enhanced tensile toughness of the material.

The tensile toughness of poly(**IBA-PDBDA**) (2% **BE**) with varying $C_{14}OH$ content was evaluated, as shown in Figure 3b (Figure S3 and Table S2). Without $C_{14}OH$, the poly(**IBA-PDBDA**) network exhibited low tensile toughness (39 kJm^{-3}), indicative of a brittle structure.

Adding $C_{14}OH$ initially led to limited improvements in toughness. However, a significant increase in toughness was observed when $C_{14}OH$ content reached 15%. At this concentration, tensile toughness surged to 3.4 MJm^{-3}, with a corresponding increase in elongation at break to 65%, representing an 8600% increase compared to the neat poly(**IBA-PDBDA**). This remarkable enhancement is attributed to phase separation and microdomain formation of $C_{14}OH$ at high concentrations (Figure 3c). As a long-chain fatty alcohol, $C_{14}OH$ likely phase-separates within the poly(**IBA-PDBDA**) matrix, creating microdomains that act as energy-absorbing sites during deformation. These domains help dissipate energy and delay crack propagation when the polymer is under stress, significantly enhancing toughness.

At lower $C_{14}OH$ concentrations, a plasticizing effect may contribute slightly to toughness, but without sufficient $C_{14}OH$ to form energy-dissipating microdomains, the improvements remain limited. Only at concentrations high enough to induce phase separation does $C_{14}OH$ exert a notable impact on toughness, underscoring the importance of reaching a threshold concentration for effective mechanical reinforcement.

The resin's performance was further optimized by adjusting **BE** content, by evaluating the mechanical properties of products with varying cross-linker content while maintaining a fixed $C_{14}OH$ content of 15%. Without any cross-linker, the polymer exhibited a storage modulus of approximately 130 MPa and an elongation at yield of 150% (Figure 4a, b and Figure S4). Introducing 1% **BE** cross-linker increased the storage modulus to 230 MPa, and the elongation at yield rose to 248%, marking a 65% improvement. This result demonstrating the superior mechanical performance typical of thermoset-like resins compared to their un-crosslinked thermoplastic counterparts.[40, 41]

Further increasing the cross-linker content (2-4%) led to a consistent reduction in elongation, from 65% for the polymer with 2% **BE** to just 6% at 4% **BE**. However, as expected, the storage modulus and tensile stress of the polymer steadily increased with higher cross-linker

concentrations (Figure 4b). This trend indicates that an increased cross-linker content raises the cross-link density and hardness of the polymer, while reducing its flexibility. The highest toughness was achieved with 1% **BE**, which was attributed to the optimal balance between structural integrity and chain mobility provided by the low level of cross-linking (Figure 4c and Table S3). At a low cross-linker concentration (1%), the polymer network is lightly cross-linked, allowing polymer chains sufficient mobility to extend under strain. This small degree of cross-linking contributes to structural integrity without overly restricting chain movement, resulting in increased elongation. As the cross-linker content increases (2-4%), the network becomes more rigid due to a higher density of covalent bonds linking the chains, which restricts chain mobility and decreases flexibility. Consequently, the polymer becomes less extensible, with elongation at yield decreasing as cross-link density increases. This behavior is corroborated by the observed increase in both storage modulus and tensile stress with higher cross-linker content.[39]

Based on the changes in tensile stress and elongation with varying cross-linker content, the tensile toughness of the polymer was mapped against different **BE** cross-linker content (Figure 4c). The result shows that the highest tensile toughness, approximately 6.2 MJm^{-3}, was achieved at a **BE** content of 1%, while toughness decreased significantly to around 0.16 MJm^{-3} at 4% **BE**. Consequently, the optimized resin with 15% $C_{14}OH$ and 1% **BE** was selected for reprocessing investigation. The FT-IR spectral analysis confirms the successful polymerization of poly(**IBA-PDBDA**) with varying **BE** content (Figure 4d). All spectra show a high conversion of the acrylate C=C bond, indicated by the distinct peak at around 1631 cm^{-1}.

We also evaluated the thermal stability of the polymer by TGA (Figure 4e). All the polymers exhibited maximum thermal decomposition at about 300 °C (corresponding to side chain and additive loss), together with further decomposition between 300 to 600 °C corresponding to

backbone C-C degradation.[42, 43] It is also worth to note that, despite the boiling point of $C_{14}OH$ being around 260 °C, there was no significant weight loss below 300 °C, even with a $C_{14}OH$ content of approximately 15%. This stability is attributed to the uniform dispersion of $C_{14}OH$ within the polymer matrix,[44] where it forms bonds with the matrix, creating microdomains, as discussed above. We were also interested in the variation of glass transition temperature with increasing crosslinker concentration. Without crosslinker (0**BE**-15$C_{14}OH$), an obvious transition temperature was observed at 93 °C. Meanwhile, for crosslinked samples, a rubbery solid was obtained after heating, which is characteristic of vitrimeric materials as the overall degree of crosslinking tends to be essentially invariant over a large temperature range due to associative dynamic crosslink exchange mechanisms.[45] In the DSC, the transition temperature was observed at 106 and 121 °C for the polymer with **BE** content of 1 and 2%. No obvious transition was observed for 4**BE**-15$C_{14}OH$ (Figure 4f). This increase in transition temperature indicates an increased restriction in segmental motion due to increased crosslinking. This result was also collaborated by our observations on a melting behaviour of the system (Figure S5), with an increase in phase transition temperature from 0**BE**-15$C_{14}OH$ to 2**BE**-15$C_{14}OH$, and no phase transition observed for 4**BE**-15$C_{14}OH$. This demonstrates that increasing crosslinking density results in an increase in glass transition temperatures due to greater molecular movement restriction. However, in this case, the values obtained were somewhat higher than those obtained on DSC. We attribute that to the difference between measurements on a macro scale, observing physical changes (on the melting point measurement system), compared to measurements on a micro scale, observing thermal changes (as observed in DSC).

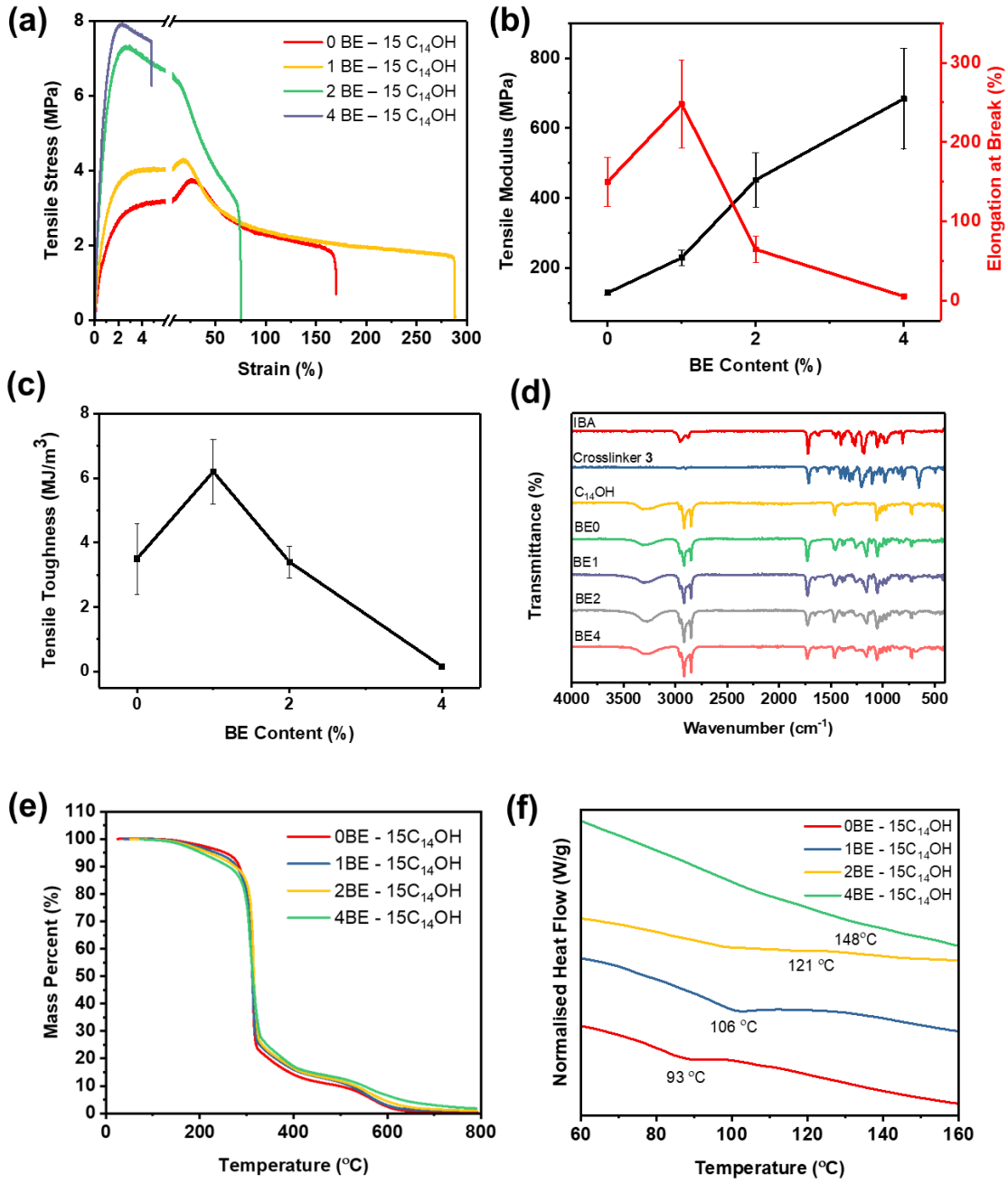

Figure 4: **Optimization of BE content in the system**. (a) Stress-strain curves of the polymer with varying amounts of **BE** (crosslinker). (b) Variation in storage modulus and elongation at yield with increasing **BE** content. (c) Tensile toughness as a function of **BE** content. (d) FT-IR spectra of poly(**IBA-PDBDA**) with different **BE** contents. (e) Thermal stability analysed using thermogravimetric analysis (TGA). (f) Transition temperature of poly(**IBA-PDBDA**) as a function of **BE** content, measured by differential scanning calorimetry (DSC).

Based on the above studies and resin optimization, we use polymer 1**BE**-15C_{14}OH as example to study the recyclability. Unlike traditional thermosets and most reported

reconfigurable resins that rely on dynamic covalent exchange, we observed a transition cycle of thermosetting-thermoplastic-thermosetting of the poly(**IBA-PDBDA**) during the re-processing. We found that 1**BE**-15C_{14}OH could be reprocessed by hot pressing (120 °C, 5 bars, 5 mins) to form uniform films, which were then die-punched into dog-bone shapes suitable for tensile testing. In contrast, films processed at 90 °C for the same duration exhibited non-uniform regions, with yellow islands indicating incomplete conversion and visible defects. Increasing the temperature to 140 °C significantly reduced the processing time, yielding a homogeneous film in just 2 minutes (Figure S6). These observations suggest that the reprocessing process is kinetically controlled. Interestingly, the reprocessed films initially displayed drastically different properties compared to the pristine samples: a significantly lower storage modulus (~60 MPa) while much higher elongation (>650%) (Figure 5a), indicating a transition from a thermoset to a thermoplastic structure. Moreover, the reprocessed sample was initially transparent, unlike the opaque pristine UV-cured sample, suggesting the formation of a more homogeneous structure. However, after one week at room temperature, the transparent samples turned opaque, likely due to the re-assembly of tetradecanol into microdomains and the reformation of boron ester cross-links with 1,2-diol groups, restoring the thermosetting structure and the reformation of phase separated tetradecanol domains. Subsequent tensile testing of these samples (after one-week post-reprocessing) showed a restored storage modulus (300 MPa, compared to ~230 MPa in pristine samples) and a reduced elongation at break (76%) (Figure 5a). An enhanced modulus as compared to the original samples was attributed to the optimized molecular packing of the resulting polymer during the re-processing process.

To further understand these changes, we conducted dynamic mechanical analysis (DMA) on the sample (1**BE**-15C_{14}OH) (Figure 5b). The freshly hot-pressed sample exhibited a transition temperature (T_g) of 53 °C, whereas the sample reprocessed one week prior showed

a T_g of 88 °C, consistent with a gradual restoration of the cross-linked thermosetting structure. Notably, both samples exhibited a similar rubbery-phase storage modulus (~0.15 MPa) at temperatures above 120 °C, indicating that that a partially crosslinked structure still exist for both samples.

Based on these observations, we propose the following mechanism (Figure 5c): At low temperatures, the polymer exhibits a typical thermosetting structure, with boron ester groups cross-linking adjacent poly**IBA** polymer chains, while tetradecanol assembles into micro/nano-domains to aid in energy dissipation. Due to the high energy required for boronic acid to react with mono-alcohol tetradecanol, the cross-linked structure remains stable. However, as temperature increases, the overall increase in energy results enables the activation energy barrier to be overcome, enabling the reaction of boronic acid with alcohol in a kinetically controlled manner. With the excess of tetradecanol present, it increasingly replaces 1,2-diol groups, disrupting cross-links and converting the thermoset structure to a partially thermoplastic one. The replacement of polymer side chains with tetradecanol also enhances compatibility, making the polymer transparent. Upon cooling, the boronic acid-alcohol reaction becomes thermodynamically controlled, selectively binding to 1,2-diol groups and restoring cross-links between the poly**IBA** backbones. Meanwhile, tetradecanol reassembles into micro/nano-domains, restoring the opaque appearance, higher modulus, and reduced elongation. These results demonstrate that the cured resin can indeed be reprocessed through hot pressing, with the material gradually regaining its original properties over time.

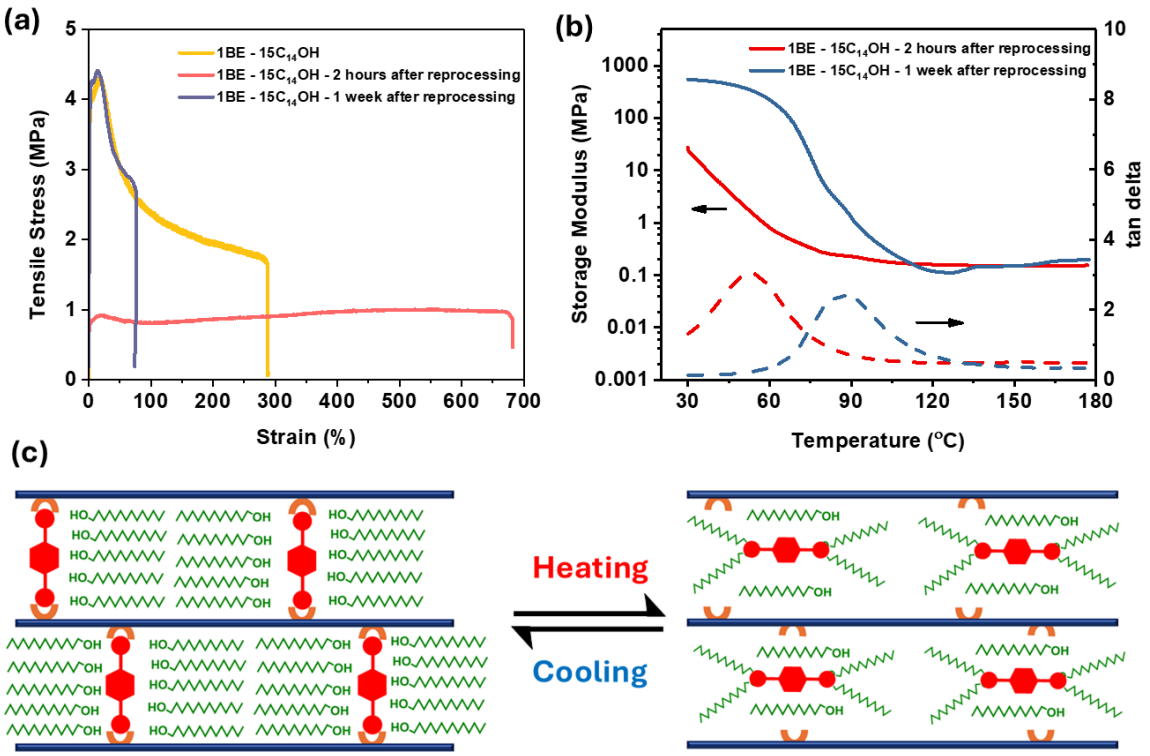

Figure 5: (a) Stress-strain relationship of pristine 1**BE**-15C_{14}OH, 2 hours after reprocessing by hot press, and 1 week after reprocessing by hot press. Insert: colour photo of 3D-printed chess piece hot-pressed into sheets, and cut into tensile bars (120 °C, 5 bars, 5 mins). (b) Change in storage modulus over temperature for samples 2 hours and 1 week after reprocessing. (c) Proposed mechanisms for the thermal levelling effect induced kinetic and dynamic boron ester reaction during the re-processing.

In this study, we developed a sustainable DLP 3D printing resin based on isobornyl acrylate (**IBA**), incorporating a diboronic ester as a cross-linker and tetradecanol as a trans-borylesterification mediator. The re-processability of the 3D-printed thermoset was achieved through trans-borylesterification, a dynamic bond exchange reaction that occurs exclusively at elevated temperatures by using the thermal levelling effect. The high temperature during reprocessing enables tetradecanol to react predominantly with boronic acid, converting the thermosetting network into a thermoplastic-like network. Upon cooling, the reaction shifts back to a thermodynamically controlled state, allowing boronic acid to selectively react with the 1,2-diol, thereby reconstructing the cross-linked thermosetting polymer network and recovering mechanical performance. Through careful optimization, the ideal resin formulation was identified as 1% boronic ester (**BE**) and 15% tetradecanol ($C_{14}OH$), balancing mechanical performance and re-processability. The proposed mechanism was validated using small-molecule models, supported by NMR analysis, which confirmed the dynamic bond exchange at 120 °C and its reversal upon cooling. The recyclability of the printed material was demonstrated by rapidly reshaping the 3D-printed parts via hot pressing at 120 °C within 5 minutes. Unlike conventional cross-linkers that create permanent topological networks, the dynamic boronic ester bonds allowed reshaping while maintaining material integrity. Although the hot-pressed samples initially exhibited lower crystallinity, glass transition temperature, and storage modulus, these properties were restored over time due to the slow trans-borylesterification at room temperature. This resin represents a step forward in sustainable 3D printing by enabling direct re-processability and end-of-life reusability, contributing to the development of a circular economy. The unique ability to transition between thermoset and thermoplastic states under controlled conditions ensures high performance and long-term material utility in DLP-based applications.

Experimental

To prepare the resin, isobornyl acrylate was mixed with 1-Tetradecanol and DMPA in a bottle with sonication at room temperature until a clear solution was obtained. The boronic ester crosslinker was then added to the resin and stirred at room temperature for 30 minutes. Finally, DPO was added to the mixture and keep stirring at room temperature for another 2 hours. The obtained resin was kept in a bottle and store in a dark place to shield from light.

UV curing of the resin was conducted in a UV oven (Asiga Flash) at room temperature for 30 minutes. The cured samples were then cleaned by sonication in isopropyl alcohol 2 times, then dried.

3D printing was conducted on a DLP printer (Asiga Pico 2). Printing was carried out with slice thickness of 50 μm. Exposure time per layer was 1.8 s. After printing, the printed part was washed thoroughly with iso-propanol, air dried and placed inside UV oven for further curing.

Detailed information about synthesis of crosslinker **3** and characterization of polymers obtained can be found in the supporting information (scheme S1).

ASSOCIATED CONTENT

Supporting Information. This material is available free of charge via the Internet at http://pubs.acs.org.

Synthetic route of crosslinker **3**. ^{1}H NMR peak intensity ratios of transesterification reaction of **BE** using different amounts of $C_{14}OH$ and correspond NMR spectra; The mechanical properties of poly(**IBA-PDBDA**) (2% **BE**) with different content of $C_{14}OH$; The mechanical properties of poly(**IBA-PDBDA**) (15% $C_{14}OH$) with different content of **BE**; Phase transition temperature of X**BE**-15$C_{14}OH$; Temperature and hot process time effect on the re-processing performance; NMR spectra of synthesized products.

AUTHOR INFORMATION

Corresponding Author

Zhuang Mao Png – Institute of Sustainability for Chemicals, Energy and Environment (ISCE2), A*STAR (Agency for Science, Technology and Research), 1 Pesek Road, Jurong Island, Singapore 627833, Republic of Singapore; ORCID: 0000-0002-4874-5234; Email: png_zhuang_mao@isce2.a-star.edu.sg.

FuKe Wang – Institute of Materials Research and Engineering, A*STAR (Agency for Science, Technology and Research), Fusionopolis Way, Innovis, #08-03, Singapore 138634, Republic of Singapore; ORCID: orcid.org/0000-0002-6980-5857; Email: wangf@imre.a-star.edu.sg

Author Contributions

All authors have given approval to the final version of the manuscript. Yi Ting Chong data curation, methodology. Suxi Wang data curation and NMR analysis; Sirawit Pruksawan data analysis and methodology; Zhuang Mao Png conceptualization, data curation, writing-original draft; Qiang Zhu and Zibiao Li writing-review and editing; FuKe Wang conceptualization, supervision, data analysis, writing and reversion.

Notes

The authors declare no competing financial interest.

ACKNOWLEDGMENT

This work was financially supported by SERC Central Research Fund (TIMR211001bSERCRF) of Agency for Science, Technology and Research (A*STAR) of Singapore and RIE2025 Manufacturing, Trade and Connectivity (MTC) Programmatic Fund. Grant No: M24N3b0028 and M22K9b0049.

REFERENCES

(1) Ligon, S. C.; Liska, R.; Stampfl, J. r.; Gurr, M.; Mülhaupt, R. Polymers for 3D printing and customized additive manufacturing. *Chemical reviews* **2017**, *117* , 10212-10290.
(2) Ma, T.; Zhang, Y.; Ruan, K.; Guo, H.; He, M.; Shi, X.; Guo, Y.; Kong, J.; Gu, J. Advances in 3D printing for polymer composites: A review. *InfoMat* **2024**, e12568.
(3) Walker, D. A.; Hedrick, J. L.; Mirkin, C. A. Rapid, large-volume, thermally controlled 3D printing using a mobile liquid interface. *Science* **2019**, *366*, 360-364.
(4) Dong, M.; Han, Y.; Hao, X. P.; Yu, H. C.; Yin, J.; Du, M.; Zheng, Q.; Wu, Z. L. Digital Light Processing 3D Printing of Tough Supramolecular Hydrogels with Sophisticated Architectures as Impact-Absorption Elements. *Advanced Materials* **2022**, *34*, 2204333.
(5) Pruksawan, S.; Chong, Y. T.; Zhao, Y.; Sivaraja, V. K.; Ngo, A. C. Y.; Jin, P.; Wang, F. Minimizing Polymer Curl Distortion and Heat Impact to Improve Digital Light Processing Printing Accuracy via Subdivision Method. *Advanced Engineering Materials*, **2024**, 2401674.
(6) Traugutt, N. A.; Mistry, D.; Luo, C.; Yu, K.; Ge, Q.; Yakacki, C. M. Liquid-crystal-elastomer-based dissipative structures by digital light processing 3D printing. *Advanced Materials* **2020**, *32*, 2000797.
(7) Caprioli, M.; Roppolo, I.; Chiappone, A.; Larush, L.; Pirri, C. F.; Magdassi, S. 3D-printed self-healing hydrogels via Digital Light Processing. *Nature communications* **2021**, *12*, 1-9.
(8) Pruksawan, S.; Lim, J. W. R.; Lee, Y. L.; Lin, Z.; Chee, H. L.; Chong, Y. T.; Chi, H.; Wang, F. Enhancing hydrogel toughness by uniform cross-linking using modified polyhedral oligomeric silsesquioxane. *Communications Materials* **2023**, *4*, 75.
(9) Zhu, G.; Houck, H. A.; Spiegel, C. A.; Selhuber-Unkel, C.; Hou, Y.; Blasco, E. Introducing dynamic bonds in light-based 3D printing. *Advanced Functional Materials* **2024**, *34*, 2300456.
(10) Jia, Y.; Xie, H.; Qian, J.; Zhang, Y.; Zheng, H.; Wei, F.; Li, Y.; Zhao, Z. Recent Progress on the 3D Printing of Dynamically Cross-Linked Polymers. *Advanced Functional Materials* **2024**, *34*, 2307279.
(11) Zhu, G.; Hou, Y.; Xiang, J.; Xu, J.; Zhao, N. Digital light processing 3D printing of healable and recyclable polymers with tailorable mechanical properties. *ACS Applied Materials & Interfaces* **2021**, *13*, 34954-34961.
(12) Maines, E. M.; Porwal, M. K.; Ellison, C. J.; Reineke, T. M. Sustainable advances in SLA/DLP 3D printing materials and processes. *Green Chemistry* **2021**, *23*, 6863-6897.
(13) Cafiso, D.; Septevani, A. A.; Noè, C.; Schiller, T.; Pirri, C. F.; Roppolo, I.; Chiappone, A. 3D printing of fully cellulose-based hydrogels by digital light processing. *Sustainable Materials and Technologies* **2022**, *32*, e00444.
(14) Wan, Z.; Zhang, H.; Niu, M.; Zhang, W.; Guo, Y.; Li, H. Development of lignin-derived UV-curable resin for DLP 3D printing. *Industrial Crops and Products* **2024**, *221*, 119243.
(15) Zhu, G.; Liu, M.; Kou, Z.; Zhang, G.; Bo, C.; Hu, L.; Hu, Y.; Zhou, Y. Universal approach for developing reprocessable and reprintable plant oil-based resins for digital light processing 3D printing. *Chemical Engineering Journal* **2023**, *475*, 146080.
(16) Chen, Z.; Yang, M.; Ji, M.; Kuang, X.; Qi, H. J.; Wang, T. Recyclable thermosetting polymers for digital light processing 3D printing. *Materials & Design* **2021**, *197*, 109189.
(17) Cui, C.; An, L.; Zhang, Z.; Ji, M.; Chen, K.; Yang, Y.; Su, Q.; Wang, F.; Cheng, Y.; Zhang, Y. Reconfigurable 4D printing of reprocessable and mechanically strong

polythiourethane covalent adaptable networks. *Advanced Functional Materials* **2022**, *32* (29), 2203720.
(18) Pruksawan, S.; Chong, Y. T.; Zen, W.; Loh, T. J. E.; Wong, J. H.; Zhu, Q.; Jin, P.; Wang, F. Sustainable Conversion of 3D-Printed Thermosets into Thermoplastics Using Methacrylic Anhydride as a Hydrolytic Cleavable Cross-Linker. *ACS Applied Polymer Materials* **2024**, *6*, 2777-2788.
(19) Zhu, G.; Hou, Y.; Xu, J.; Zhao, N. Reprintable polymers for digital light processing 3D printing. *Advanced Functional Materials* **2021**, *31*, 2007173.
(20) Alim, M. D.; Childress, K. K.; Baugh, N. J.; Martinez, A. M.; Davenport, A.; Fairbanks, B. D.; McBride, M. K.; Worrell, B. T.; Stansbury, J. W.; McLeod, R. R. A photopolymerizable thermoplastic with tunable mechanical performance. *Materials Horizons* **2020**, *7*, 835-842.
(21) Childress, K. K.; Alim, M. D.; Hernandez, J. J.; Stansbury, J. W.; Bowman, C. N. Additive manufacture of lightly crosslinked semicrystalline thiol–enes for enhanced mechanical performance. *Polymer chemistry* **2020**, *11*, 39-46.
(22) Zhu, G.; von Coelln, N.; Hou, Y.; Vazquez-Martel, C.; Spiegel, C. A.; Tegeder, P.; Blasco, E. Digital Light 3D Printing of Double Thermoplastics with Customizable Mechanical Properties and Versatile Reprocessability. *Advanced Materials* **2024**, *36*, 2401561.
(23) Fang, Z.; Shi, Y.; Mu, H.; Lu, R.; Wu, J.; Xie, T. 3D printing of dynamic covalent polymer network with on-demand geometric and mechanical reprogrammability. *Nature Communications* **2023**, *14*, 1313.
(24) Robinson, L. L.; Self, J. L.; Fusi, A. D.; Bates, M. W.; Read de Alaniz, J.; Hawker, C. J.; Bates, C. M.; Sample, C. S. Chemical and mechanical tunability of 3D-printed dynamic covalent networks based on boronate esters. *ACS Macro Letters* **2021**, *10*, 857-863.
(25) Bijalwan, V.; Rana, S.; Yun, G. J.; Singh, K. P.; Jamil, M.; Schlögl, S. 3D Printing of Covalent Adaptable Networks: Overview, Applications and Future Prospects. *Polymer Reviews* **2024**, *64*, 36-79.
(26) Krishna Kumar, B.; Dickens, T. J. Dynamic bond exchangeable thermoset vitrimers in 3D-printing. *Journal of Applied Polymer Science* **2023**, *140*, e53304.
(27) Cortés-Guzmán, K. P.; Parikh, A. R.; Sparacin, M. L.; Remy, A. K.; Adegoke, L.; Chitrakar, C.; Ecker, M.; Voit, W. E.; Smaldone, R. A. Recyclable, biobased photoresins for 3d printing through dynamic imine exchange. *ACS Sustainable Chemistry & Engineering* **2022**, *10*, 13091-13099.
(28) Stouten, J.; Schnelting, G. H.; Hul, J.; Sijstermans, N.; Janssen, K.; Darikwa, T.; Ye, C.; Loos, K.; Voet, V. S.; Bernaerts, K. V. Biobased photopolymer Resin for 3D printing containing dynamic imine bonds for fast reprocessability. *ACS Applied Materials & Interfaces* **2023**, *15*, 27110-27119.
(29) Wang, L.; Zhang, K.; Zhang, X.; Tan, Y.; Guo, L.; Xia, Y.; Wang, X. Mismatched Supramolecular Interactions Facilitate the Reprocessing of Super-Strong and Ultratough Thermoset Elastomers. *Advanced Materials* **2024**, *36*, 2311758.
(30) Cho, S.; Hwang, S. Y.; Oh, D. X.; Park, J. Recent progress in self-healing polymers and hydrogels based on reversible dynamic B–O bonds: boronic/boronate esters, borax, and benzoxaborole. *Journal of Materials Chemistry A* **2021**, *9*, 14630-14655.
(31) Teotonico, J.; Mantione, D.; Ballester-Bayarri, L.; Ximenis, M.; Sardon, H.; Ballard, N.; Ruipérez, F. A combined computational and experimental study of metathesis and

nucleophile-mediated exchange mechanisms in boronic ester-containing vitrimers. *Polymer Chemistry* **2024**, *15*, 181-192.
(32) Fang, Z.; Shi, Y.; Zhang, Y.; Zhao, Q.; Wu, J. Reconfigurable polymer networks for digital light processing 3D printing. *ACS Applied Materials & Interfaces* **2021**, *13*, 15584-15590.
(33) Roy, C. D.; Brown, H. C. Stability of boronic esters–Structural effects on the relative rates of transesterification of 2-(phenyl)-1, 3, 2-dioxaborolane. *Journal of Organometallic Chemistry* **2007**, *692*, 784-790.
(34) Sinawehl, L.; Wolff, R.; Koch, T.; Stampfl, J. r.; Liska, R.; Baudis, S. Photopolymers based on boronic esters for the enhanced degradation of 3D-printed scaffolds. *ACS Applied Polymer Materials* **2023**, *5*, 5758-5771.
(35) Zhang, C.; Yang, Z.; Duong, N. T.; Li, X.; Nishiyama, Y.; Wu, Q.; Zhang, R.; Sun, P. Using dynamic bonds to enhance the mechanical performance: from microscopic molecular interactions to macroscopic properties. *Macromolecules* **2019**, *52*, 5014-5025.
(36) Chen, Y.; Tang, Z.; Zhang, X.; Liu, Y.; Wu, S.; Guo, B. Covalently cross-linked elastomers with self-healing and malleable abilities enabled by boronic ester bonds. *ACS applied materials & interfaces* **2018**, *10*, 24224-24231.
(37) Tajbakhsh, S.; Hajiali, F.; Guinan, K.; Marić, M. Highly reprocessable, room temperature self-healable bio-based materials with boronic-ester dynamic cross-linking. *Reactive and Functional Polymers* **2021**, *158*, 104794.
(38) Jakubowski, W.; Juhari, A.; Best, A.; Koynov, K.; Pakula, T.; Matyjaszewski, K. Comparison of thermomechanical properties of statistical, gradient and block copolymers of isobornyl acrylate and n-butyl acrylate with various acrylate homopolymers. *Polymer* **2008**, *49*, 1567-1578.
(39) López-García, M. d. C.; Beebe, D.; Crone, W. Characterization of poly (isobornyl acrylate) as a construction material for microfluidic applications. *Journal of applied polymer science* **2007**, *105*, 1894-1902.
(40) Lee, Z. Y.; Kamarulzaman, S.; Rasyiddin, R.; Sim, S. Y.; Seah, G. E.; Gan, A. W.; Li, Z.; Png, Z. M.; Goh, S. S. Dynamic crosslinking of thermoplastics via perfluorophenyl nitrene C–H insertion to form recyclable thermosets. *Chem* **2025**, in press, https://doi.org/10.1016/j.chempr.2025.102479.
(41) Chiou, B. S.; Schoen, P. E. Effects of crosslinking on thermal and mechanical properties of polyurethanes. *Journal of applied polymer science* **2002**, *83*, 212-223.
(42) Manring, L. E. Thermal degradation of poly (methyl methacrylate). 2. Vinyl-terminated polymer. *Macromolecules* **1989**, *22* (6), 2673-2677.
(43) Manring, L. E.; Sogah, D. Y.; Cohen, G. M. Thermal degradation of poly (methyl methacrylate). 3. Polymer with head-to-head linkages. *Macromolecules* **1989**, *22*, 4652-4654.
(44) Choi, J.; Fujita, H.; Ogura, M.; Sakoda, A. Confinement effect on enthalpy of fusion and melting point of organic phase change materials in cylindrical nanospace of mesoporous silica and carbon. *Adsorption* **2018**, *24*, 345-355.
(45) Krishnakumar, B.; Sanka, R. P.; Binder, W. H.; Parthasarthy, V.; Rana, S.; Karak, N. Vitrimers: Associative dynamic covalent adaptive networks in thermoset polymers. *Chemical Engineering Journal* **2020**, *385*, 123820.

Table of Contents

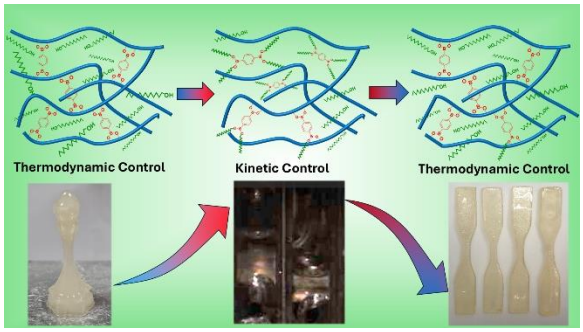
Thermodynamic Control
Kinetic Control
Thermodynamic Control